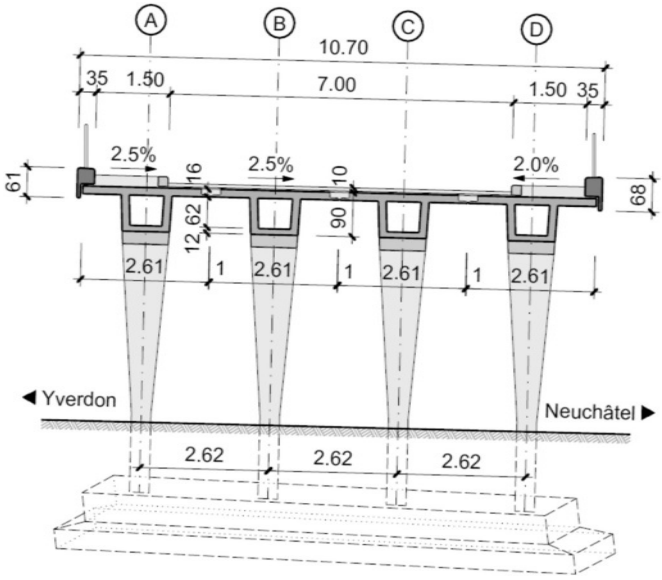

Fig. 17. Transversal section of the Grandson bridge.

Table 3
Material characteristics deducted from the standards of the time.

Element Type	$f_{cd,28}$ (MPa)	EM (MPa)	f_{yk} (MPa)	F_p (kN)	Regulation
Fondations	29.42	33,402	–	–	[61,62]
Piles	47.07	36,982	–	–	[61,62]
Bridge deck	47.07	36,982	–	–	[61,62]
Steel bars	–	–	450	–	[61,62]
Adherent wires	–	–	1500	44.52	[61,62]
Post-prestressed cables	–	–	1550	1255.25	[61,62]

$f_{cd,28}$: Design 28-days compressive strength; EM: Elastic Modulus; f_{yk}: Characteristic yield strength; F_p: Prestressing force.

Fig. 18. The geometrical characteristics of the truck can be found in Fig. 19. The load magnitude was chosen to ensure measurable deformations. Measurement points are positioned at the midpoint of the bridge, where deformations are greatest, thereby minimizing the impact of inherent measurement errors.

Three different technologies have been employed to measure the displacement field for three different load conditions: (i) high precision leveling, (ii) total station measurements and (iii) DIC.

The first two techniques were chosen for their widespread use in surveying, enabling measurement of vertical deflection and horizontal displacement. DIC was selected for its emerging reputation as a cost-effective solution. DIC involves analyzing digital images taken at different times to detect displacements using affordable cameras [63–66]. Despite being widely used in laboratories [67,68], a challenge is the impact of camera movement on measured quantities [69]. DIC has successfully monitored deformations in structures and studied degradation phenomena, including corrosion of rebars [70–72]. However, the use of some commercial DIC systems must be carefully evaluated when varying lighting conditions, occurs, since further algorithmic calculations might be necessary [73].

The leveling network was surveyed and included four control points (outside of the measurement area) using a digital level (NA03 by Leica Geosystems) and an invar staff to minimize any thermal deformations which could compromise the quality of the measurements [74], see Fig. 18. The displacement field is evaluated for each load combination at the labeled points P2 and P5 as reported in Fig. 18.

Two total stations (MS50 by Leica Geosystems) were installed outside of the measurement area on the northern side of the bridge in order to measure the points displacements, in which are placed the targets, see Figs. 18 and 20. Control points were used to check the stability of both, the digital levels and the total stations. This correction has been taken into account in Section 4.5.1.

The DIC technology is used to evaluate the entire vertical displacement of the bridge deck for both sides of the bridge. Images were captured by one Canon EOS 5D Mark III with 50 mm focal length. This device has been installed so as to remain as stable as possible between shots, see Fig. 21. Shooting parameters were set so as to obtain the best signal to noise ratio, with intensity levels close to saturation on the deck of the bridge. The arrangement of cameras and measured points of the three different technologies is shown in Fig. 18.

In order to know the pixel size of the DIC measurements, bridge length was measured with both techniques: total stations and DIC. The ratio between the number of pixels separating these two points in the

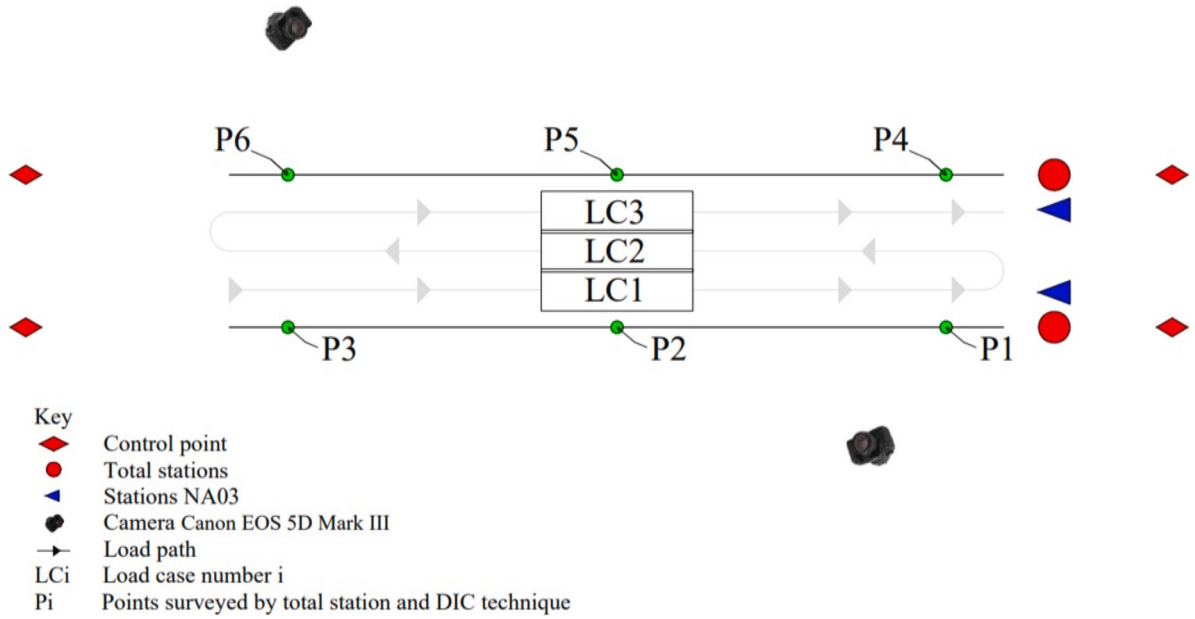

Fig. 18. Load case disposition and the set up for the surveying measurements.

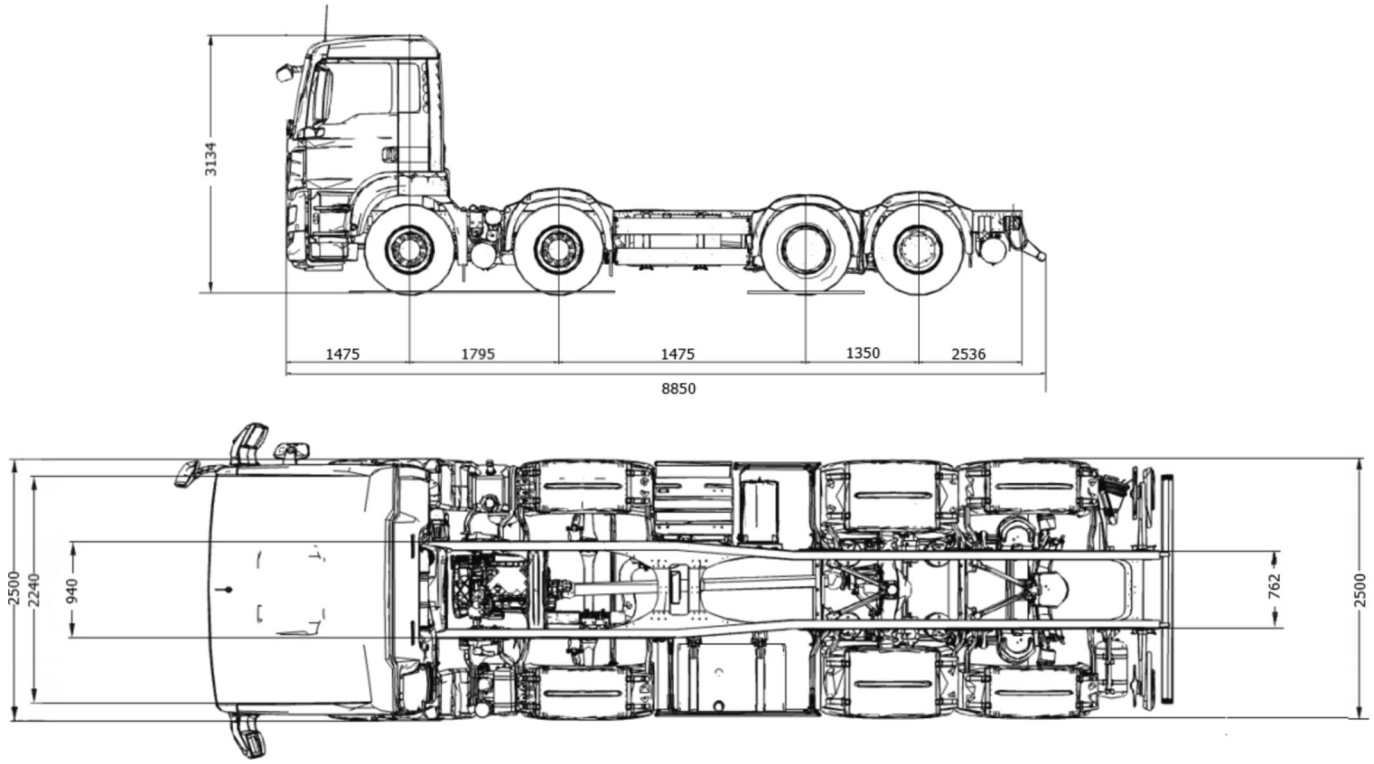

Fig. 19. Geometrical characteristic of the truck (dimensions in mm).

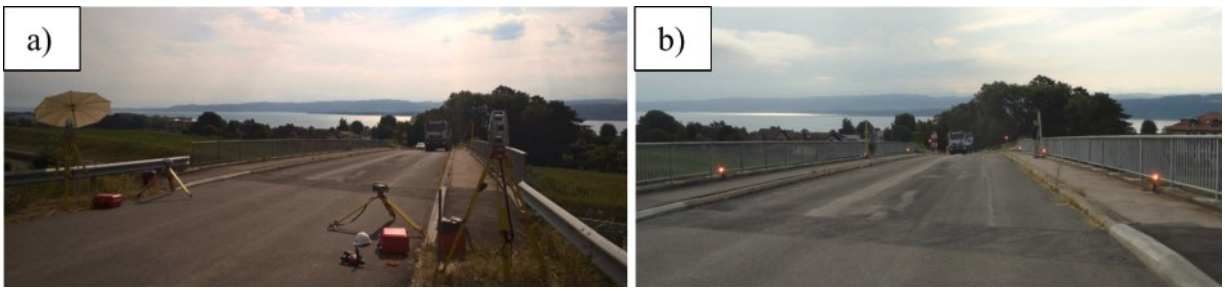

Fig. 20. a) Total station and digital level location, b) Target point location Pi.

Fig. 21. DIC measurements.

image and the metric distance returns the scaling factor. During the data processing a mask delimitation is made to evaluate the correlation, see Fig. 22. Correlation is made via an open source software "MicMac" [75], the main implemented correlation factors are reported in Table 4. In fact, points measured with the DIC refer to the mask and have been taken as close as possible in the position of the target points where receivers were located (see Fig. 18). The precision achieved is of the order of 0.01 mm.

The visualizations were performed with the SAGA GIS software [76]. A translation of the second image has been undertaken for several steps, as it is often observed that both images experience slight shifts of up to 5 pixels. Translation values are resulting from the Helmert calculation. This provides a homogeneous translation, a factor scale and a rotation between the reference image and the distorted one, see Eq. (1)

$$P = sQR + \nu T^T \tag{1}$$

where

$$R = \begin{bmatrix} 1 & \theta_3 & -\theta_2 \\ -\theta_3 & 1 & \theta_1 \\ \theta_2 & -\theta_1 & 1 \end{bmatrix}$$

Fig. 22. Mask definition for the correlation evaluation.

Table 4
Implemented correlation parameter.

Parameters	Settings
Correlation window size	10 plxs
Minimum correlation coefficient	0.98
Correlation range	0.02–1 plxs
Regularization coefficient	0.01

s is the scale factor, $R \in R^{3\times3}$ is a rotation matrix, ν is an n-length vector and T is $R^{3\times1}$ translation matrix. Translation correction provides regular results; in fact, this solution is preferred instead of modifying the calculation parameters between different images in pairs.

4.4. Finite element model (grandson bridge)

A Finite Element (FE) model of the Grandson bridge was manually created, with SCIA Engineer software [47], in order to compare the acquired results with those extracted from the structural analysis. It can be observed that, in comparison to the previous case study (see Section 3.5), the absence of interoperability or an existing DT imposes a significant constraint on modeling efficiency. Indeed, although the Praz Bridge case required some manual operations, these were minimal.

The FE model is compliant with the geometric characteristics reported in Figs. 16 and 17 and calibrated accordingly to the materials parameters reported in Table 3. The piles are modelled as 1D-beam elements. Both, the caisson beams and the slab, are modelled through 2D shell elements that are subjected to an average size mesh refinement of 250 mm. A fixed constrain condition is applied at the base of the structure. This seems to be reasonable because of the foundations dimension. Fig. 23 shows the solid and the single-line FE model views.

The static load is modelled according to the trucks' technical specification, see Fig. 19. The total load of 21.995 ton is applied following an appropriate distribution: each wheel is considered to have a load footprint of 40 × 40 cm. A further load sharing is made by following an inclination of 45° until the slab half thickness [48], see Fig. 24. Fig. 25

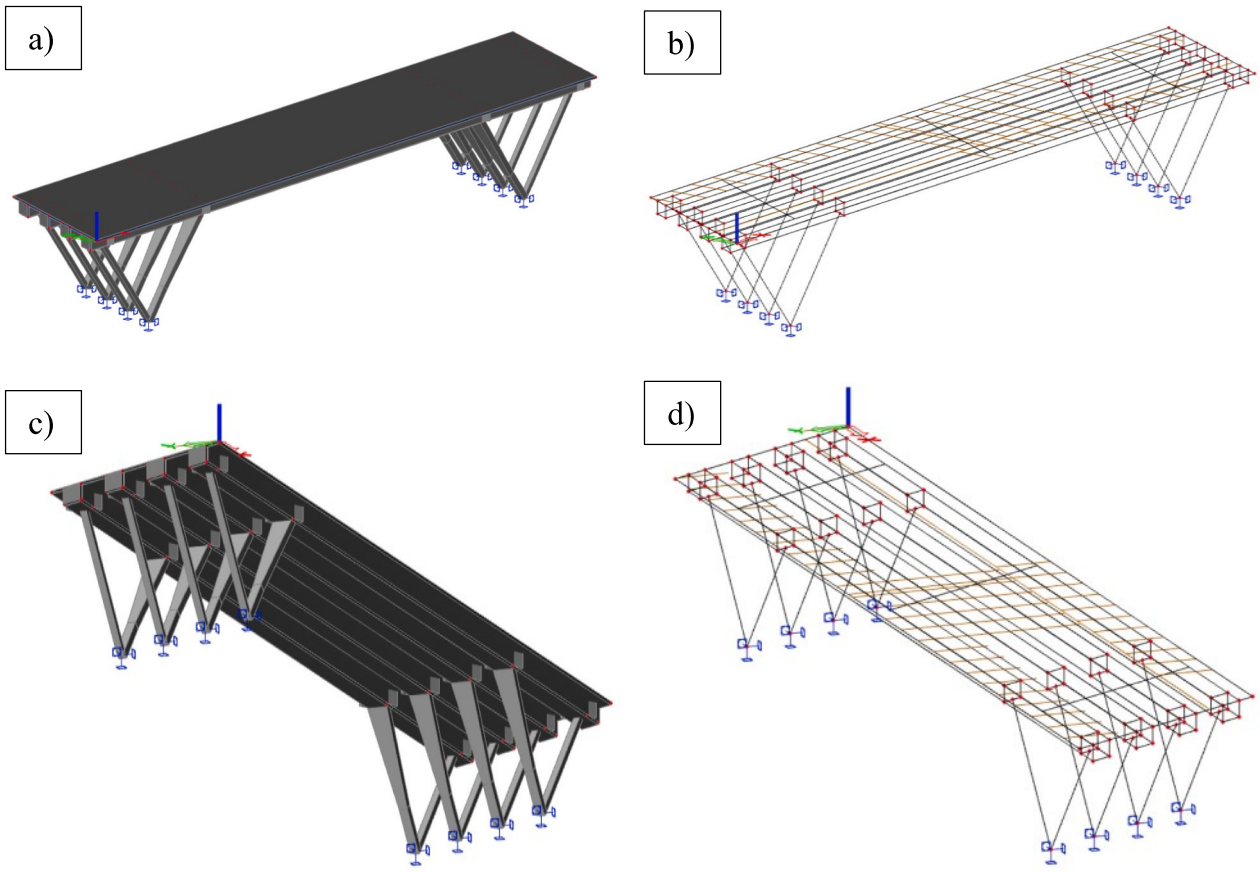

Fig. 23. FE model (Grandson bridge): a) solid view from the top, b) single-line view from the top, c) solid view from the bottom, d) single-line view from the bottom.

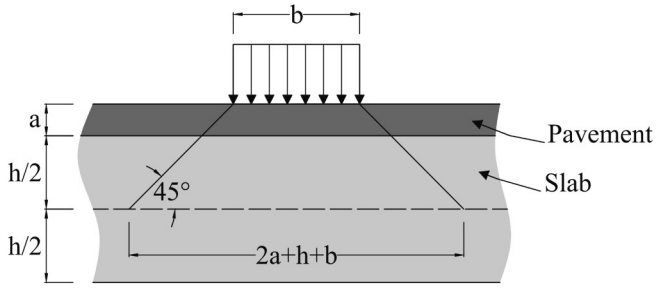

Fig. 24. Load diffusion in a slab [48].

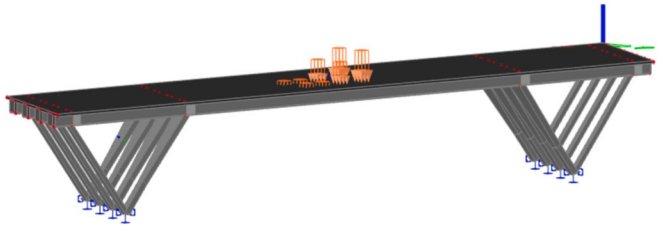

Fig. 25. First load case (LC1).

reports the first load case disposition.

Although this model respects the dictates of the time, it does not represent faithfully the real stiffness, the geometries, and the materials used. Such differences lead to results that render the predictive model unsuitable for monitoring purposes. This can be compensated by an optimization process.

In order to update the FE model, the problem is first simplified, leading to an optimized law while maintaining computational efficiency. The proposed approach relies on the static scheme illustrated in Fig. 26. Displacement values at points P1-P6, indicated in Fig. 26, were computed assuming the bridge deck as a Timoshenko beam element. The displacement functions S_a, S_b, and S_c have been expressed in function of: the (i) elastic modulus (EM), (ii) the first span length (L_a), and (iii) the middle span length (L_b). These are the key variables to be optimized. According to [77], optimization parameters might include material characteristics, geometric features, and masses. The EM was chosen for its significant influence on the entire structure, along with L_a and L_b for taking into account potential asymmetries. L affects deflection with a power of 3, while self-weight, EM and inertia with a power of 1. Notably, not all software allows inertia variation without altering the cross-section. The DE algorithm implemented facilitates escaping local minima, but the optimized solution may deviate significantly from initial values if parameters that strongly impact control parameters (S_a, S_b and S_c) are not used. However, optimization parameters choice also depends on the model's objectives and the structure type. The DE algorithm is implemented in Wolfram Mathematica platform [78]. The optimization process entails minimizing the objective function, obtained as the sum of squared differences between measured (mean of DIC measurements for all loading conditions for each midspan) the

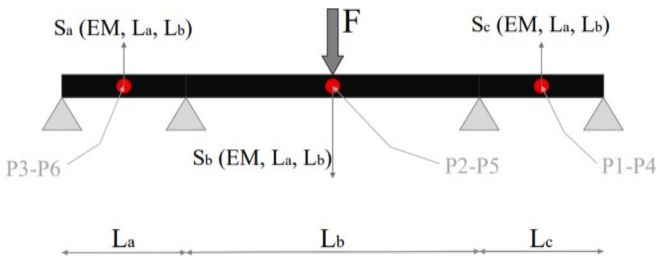

Fig. 26. Simplified static diagram for the FE model optimization.

calculated values using the displacement functions S_a, S_b, and S_c.

4.5. Digital twins vs. outdated bridge models: Insights from the grandson bridge example

The subsequent sections detail the results of an updated finite element model (FEM_U) developed for monitoring purposes. Although this model accurately reflects the bridge's condition at a specific moment, it does not include periodic updates necessary to capture the ongoing progression of bridge degradation. Consequently, an additional section explores the application of DT for real-time monitoring, utilizing models from existing Literature, to address the limitations of the outdated model.

4.5.1. In-situ measurements

Initially, the results from in-situ measurements are presented to: (i) validate the accuracy of DIC as a displacement measurement tool, and (ii) establish reference parameters for calibrating an optimized FE model.

A comparison between the displacements measured by the three different acquisition systems is reported in Fig. 27. For the sake of clarity the acronym LCi TS/DIC/L refers to the i-th load case (LCi), for the respective technologies of Total Station (TS), Digital Image Correlation (DIC), and high-precision level (L).

From the two digital levels (NA03), displacement measurements were made on both P2 and P5 and the deviations between the initial and final discharge condition calculated. These differences are used to compensate the measurements.

It is possible to note that the discrepancies between the observed values are acceptable, in particular when considering those obtained using the DIC method. This is due to the fact that the DIC measurements are taken on the bridge deck, which does not have precisely the same measured points as other methods, even if they are very close. It should be noted that the downward displacements have a negative sign. These results suggest how the use of a cost-effective technology like DIC can be easily employed for monitoring small structures, while still achieving a good approximation of the measured results.

4.5.2. FE model optimization with DIC measurements

Starting from the average DIC displacement results for each midspan the optimization of the FE model has been made manually using the DE algorithm to determine the global minimum of the objective function obtained as described in Section 4.4. To ensure physically meaningful solutions, the values of L_a and L_b were constrained between 9 and 12 m and 26 and 30 m, respectively. After multiple iterations, the optimal values of EM, L_a, and L_b were obtained as 67,432.7 MPa, 9 m, and 30 m. In Fig. 28, the iterative process followed to determine the most suitable parameters is depicted.

Fig. 29 presents the comparison between the results of the non-optimized model (FEM), FEM_U, and DIC vertical deflection measurements. It is possible to observe that displacements calculated using the non-optimized model are significantly larger, reaching up to three times the DIC values measured. This implies that compared to conventional modeling the reality appears to be much stiffer. This is caused by a combination of two factors: (i) the materials effectively used were more performant than those declared (this has a direct influence on EM used) and (ii) the model does not consider the rigidity offered by some non-structural element such as the pavement and the curbs. Instead, the FEM_U accurately captures the DIC measured displacements with average low errors.

These turn out to be suitable for the purpose, mainly because a simplified model with few variables was utilized to achieve computational efficiency in the optimization of the FE model. The points with the smallest error are prime candidates for sensor placement in potential real-time monitoring systems. In Fig. 30, a schematic illustration of the midspan displacement values obtained through DIC, FEM_U and FEM is

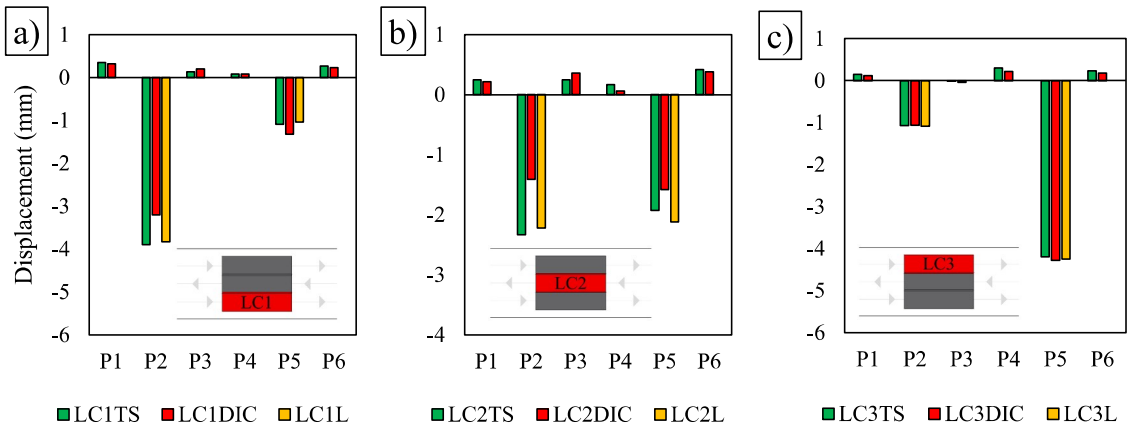

Fig. 27. Comparison of midspan displacements measured by different techniques for: a) LC1, b) LC2, and c) LC3.

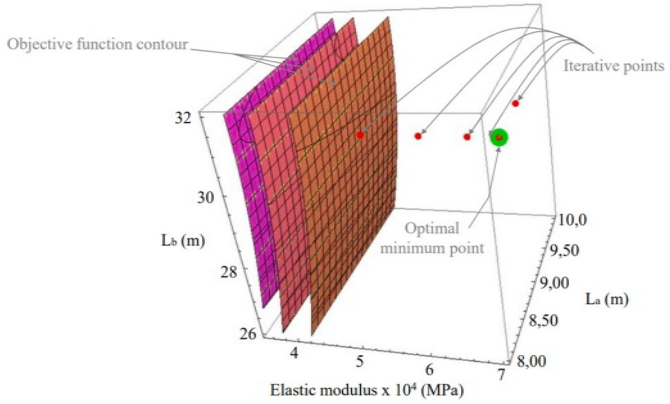

Fig. 28. FE model updating process through the differential evolution algorithm.

shown. The deformations were obtained using interpolation laws. The percentage deviations are referenced to the DIC measurement, serving as a comparative benchmark. A certain asymmetry can be observed both longitudinally and transversely. This aspect was already captured by the non-optimized model, highlighting the appropriateness of the geometry implemented in the FE model even in the absence of a scanning survey. Nevertheless, by using L_a as an optimization parameter, FEM_U allows to better capture the longitudinal asymmetric behavior. Instead, the transverse behavior was not considered in the optimization process since the optimization function was written for a beam Timoshenko element. To achieve better accordance, the optimization function should be based on bending plates solution, taking into account the deformability of the V-shaped piles, and considering more optimization parameters. However, this would result in a significant increase in computational effort, compromising the cost-effectiveness aim.

4.5.3. *Leveraging DT and optimized FEM for teal-time monitoring*

At present, the data from this case and the prepared model could be fully recovered only because the software developers and FE model designers are authors of this paper or members of the same institution. Additionally, the version of the software used to construct the FE model is still available on the institution's servers. A competent engineer who did not participate in this research or who only had access to the dataset without the proprietary software would not have been able to retrieve the relevant information. Moreover, the bridge, which was recently refurbished at the time, may exhibit different behavior today, by instance due to degradation phenomena or geotechnical issues.

While this method is effective in the short term, it faces several challenges regarding long-term viability. Firstly, the issue of software obsolescence arises, as the software may become outdated or unavailable within a few years. Additionally, the model requires manual updates based on inspections conducted by specialized operators. In contrast, a DT similar to the one used for the Praz Bridge can mitigate these issues by: (i) offering interoperability and resistance to obsolescence, and (ii) facilitating more efficient model optimization through tools such as degradation visualization (see Figs. 10–11). Moreover, the DT interfaces with a system that leverages data from a cost-effective DIC system, which identifies abnormal displacements through image acquisition and measurement. This can be achieved by following a

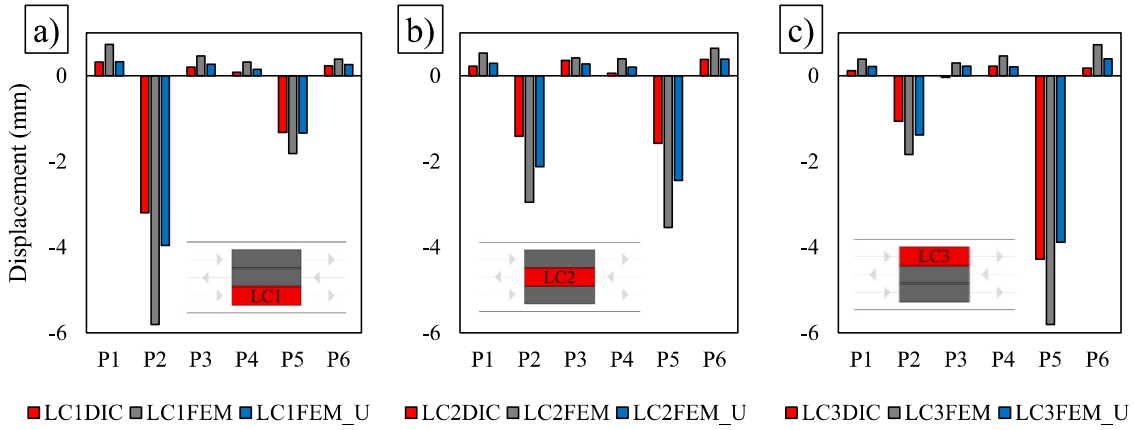

Fig. 29. Comparison of point displacements on the bridge deck for: a) LC1, b) LC2, and c) LC3.

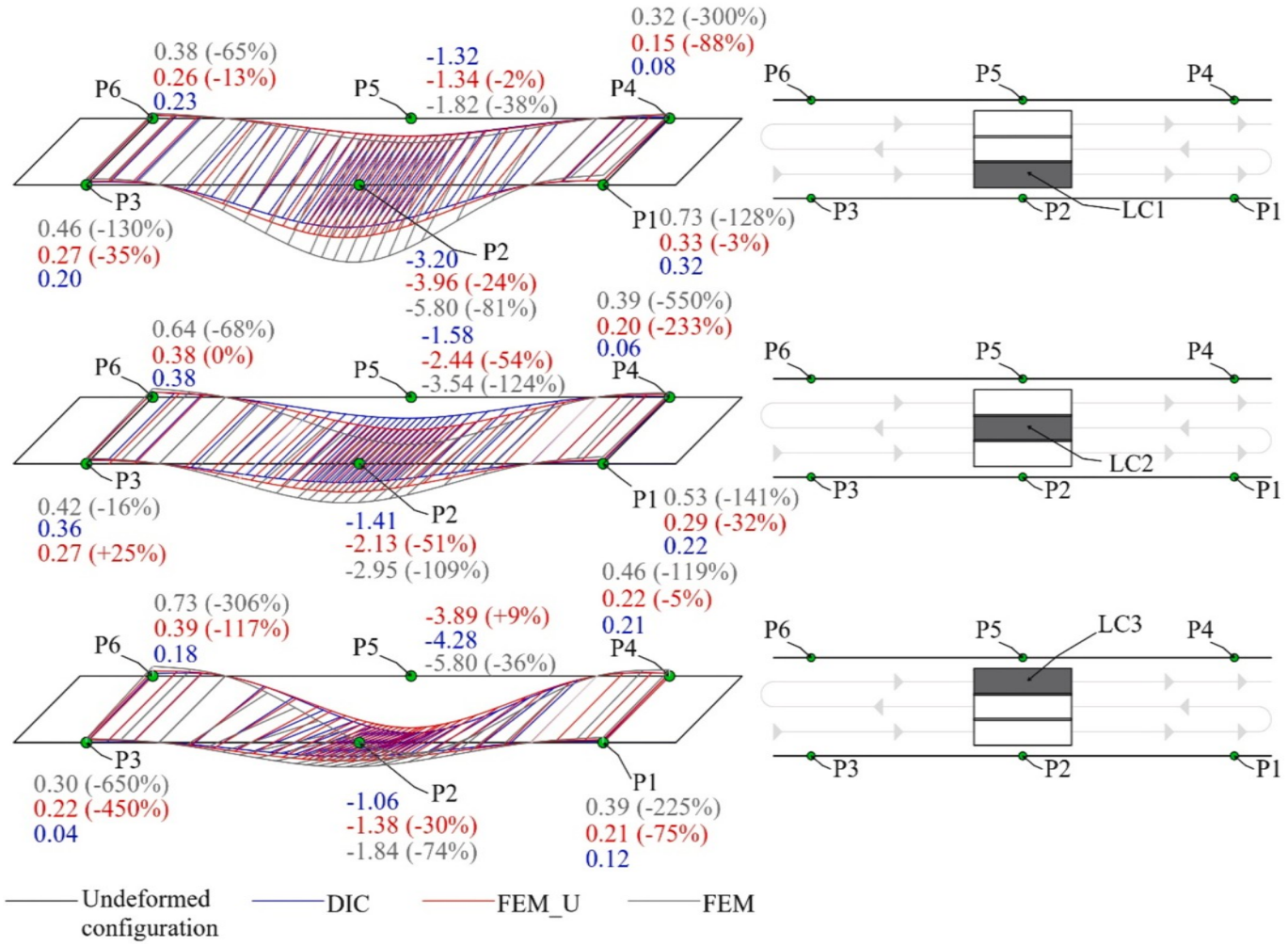

Fig. 30. Comparison of the deformed configuration evaluated with DIC, FEM and FEM_U for each load condition.

similar pattern to that presented in [36], see Fig. 31. In Phase 1, the FE model undergoes optimization using parameters defined by the DE algorithm. Various load combinations are applied to reach ULS [48], and permissible deflection values are established at critical points. In Phase 2, the predicted results are compared with field measurements under current conditions to assess changes in the target bridge object's condition.

This enables the transition to a DT at higher levels of maturity, as it has a direct real-time connection with the physical object and can inform inspectors immediately upon detecting an abnormal deflection.

Meanwhile, the DT, coupled with the continuous monitoring system, would enable inspectors to oversee a large number of structures without needing to move unless urgent or planned inspections are scheduled.

5. Conclusions and future work

This paper presents a comprehensive methodology for developing and utilizing Digital Twin (DT) models for existing bridges. Key elements of this methodology include the integration of Building Information Modeling (BIM), open-access interoperable formats, and a

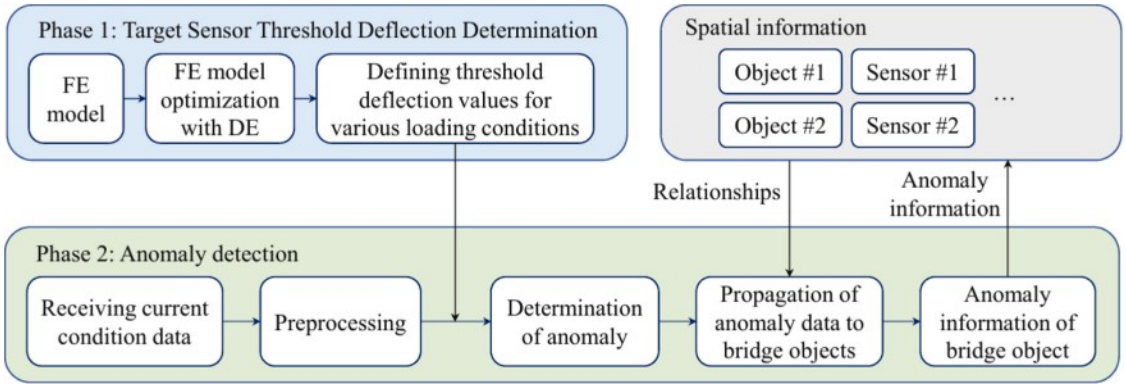

Fig. 31. Method for monitoring bridge elements using optimized FE model.

specific ontology. This approach ensures that DTs accurately reflect the current state of the bridge and can incorporate past and future inspections and monitoring results. It facilitates precise assessments of structural health and its evolution over time, enabling optimal management of maintenance operations. Additionally, the methodology promotes collaboration among professionals, aiding bridge owners in knowledge sharing, cost reduction, safety enhancement, and addressing the obsolescence typical of non-interoperable digital models.

Key findings of this paper include:

1. Existing Bridges: For medium and large bridges, converting a laser-scanned 3D model into a digital twin using Industry Foundation Classes (IFC) protocols is feasible and time-efficient, though not fully automatic. These DTs enable "what if" scenario analyses, supporting more strategic and sustainable maintenance decisions.
2. Importance of Ontology and Interoperability: The effectiveness of a DT for bridge owners depends on its ontology, interoperability, openness, and ability to integrate results from ongoing structural health monitoring. These factors ensure that the DT remains a valuable tool throughout its lifecycle and is not prone to obsolescence.
3. Sustainability: This methodology supports sustainability throughout the bridge's lifecycle by enabling data-driven planning for deconstruction, reuse, and recycling at the end of its service life. More precise management of maintenance operations and the evolution of structural health can increase the lifespan of a bridge.

Research is underway, and future work is planned to address the following challenges and enhance the impact of DTs:

1. Integration of Inspection and Monitoring Results: Often, bridge owners have internal departments and protocols to identify, classify, rate, group, and insert into a database the parameters and degradation factors that influence the structural health of a bridge. Therefore, incorporating these parameters into a newly created DT is as seamless and efficient as the internal organization managing these issues. A new method should be developed to collect and organize data in a way that ensures efficiency and accuracy.
2. Applicability to New Bridges and Structures: The strategies discussed for constructing DTs are likely to be applicable to new bridges and structures, optimizing sustainability-based design. To be effective, DTs must be used during the design phase by all professionals involved and must be able to compute emissions, energy consumption, and waste throughout the entire construction process, including the supply chain.
3. Integration into a DT Network: DTs built with this methodology can be integrated into a broader network, enabling effective management of interactions between the bridge and its environment. However, the concept of collaborating DTs is still the subject of intense research, and a debate on the level of automation to be allowed in a network of DTs has not yet surfaced.

In summary, this work represents a significant advancement in the digitalization of bridges within a "cradle-to-cradle" framework, with the potential to streamline life cycle management, address software obsolescence, and ensure optimal longevity of structures. While the proposed methodology for building bridge DTs has proven effective in simplifying structural health assessments and enhancing maintenance decision-making, further research is needed to maximize its impact, particularly by simplifying the integration of inspection and monitoring results into DTs. Future work should focus on extending this methodology to other applications, such as optimizing the environmental impact of new constructions during the design phase. Additionally, research is necessary to explore the potential of integrating similarly constructed DTs into a network, enabling the modeling of entire transportation corridors and the territories in which they are situated.

CRediT authorship contribution statement

M. Franciosi: Writing – original draft, Software, Methodology, Investigation. **M. Kasser:** Writing – review & editing, Validation, Supervision. **M. Viviani:** Writing – review & editing, Validation, Supervision, Funding acquisition.

Declaration of competing interest

The authors declare that they have no known competing financial interests or personal relationships that could have appeared to influence the work reported in this paper.

Data availability

The raw/processed data required to reproduce these findings cannot be shared at this time as the data also forms part of an ongoing study.

Acknowledgments

This research is supported by the HES-SO, University of Applied Sciences and Arts Western Switzerland in the frame of the project "BridgeTwin", a collaboration between the Haute École du Paysage, d'Ingénierie et d'Architecture de Genève (HES-SO / HEPIA) and Haute École d'Ingénierie et de Gestion du canton de Vaud (HES-SO / HEIG-VD). The authors would also like to express gratitude to the Swiss Federal Roads Office (ASTRA/OFROU) for their valuable insights on the database and case studies. Authors also acknowledge Prof. B. Domer, Y. Schatz, F. Boujon, Prof. B. Cannelle, K. Morel and V. Savino who actively contributed to the development of the digital twins.

References

[1] K.H. LeBeau, S.J. Wadia-Fascetti, Fault tree analysis of Schoharie Creek bridge collapse, J. Perform. Constr. Facil. 21 (2007) 320–326, https://doi.org/10.1061/(ASCE)0887-3828(2007)21:4(320).
[2] A.C. Estes, D.M. Frangopol, Bridge lifetime system reliability under multiple limit states, J. Bridg. Eng. 6 (2001) 523–528, https://doi.org/10.1061/(ASCE)1084-0702(2001)6:6(523).
[3] A. Contin, E. Viviani, M. Viviani, New Po River bridge at Piacenza, Italy: the construction process, Struct. Eng. Int. 21 (2011) 433–436, https://doi.org/10.2749/101686611X13131377725523.
[4] N. Rania, I. Coppola, F. Martorana, L. Migliorini, The collapse of the Morandi bridge in Genoa on 14 august 2018: a collective traumatic event and its emotional impact linked to the place and loss of a symbol, Sustainability 11 (2019) 6822, https://doi.org/10.3390/su11236822.
[5] J. Golden, E. Gomes, Anurag Roy, Y.T. Su, De La Concorde Overpass Bridge Collapse: Analysis of a Historical Failure, 2018, https://doi.org/10.13140/RG.2.2.17401.01129.
[6] M.V. Biezma, F. Schanack, Collapse of steel bridges, J. Perform. Constr. Facil. 21 (2007) 398–405, https://doi.org/10.1061/(ASCE)0887-3828(2007)21:5(398).
[7] J.S. Kong, D.M. Frangopol, Probabilistic optimization of aging structures considering maintenance and failure costs, J. Struct. Eng. 131 (2005) 600–616, https://doi.org/10.1061/(ASCE)0733-9445(2005)131:4(600).
[8] S. Kim, D.M. Frangopol, M. Soliman, Generalized probabilistic framework for optimum inspection and maintenance planning, J. Struct. Eng. 139 (2013) 435–447, https://doi.org/10.1061/(ASCE)ST.1943-541X.0000676.
[9] L. Deng, W. Wang, Y. Yu, State-of-the-art review on the causes and mechanisms of bridge collapse, J. Perform. Constr. Facil. 30 (2016) 04015005, https://doi.org/10.1061/(ASCE)CF.1943-5509.0000731.
[10] A. Contin, E. Viviani, M. Cavetti, M. Viviani, Testing, maintenance and reinforcement of the Pietrastretta RA05 motorway viaduct, in: Concr. Repair Rehabil. Retrofit. III, CRC Press, Cape Town, South Africa, 2012, pp. 293–294, https://www.taylorfrancis.com/chapters/edit/10.1201/b12750-135/testing-maintenance-reinforcement-pietrastretta-ra05-motorway-viaduct-contin-viviani-cavetti-viviani.
[11] M. Viviani, E. Viviani, A. Mardegan, A. Contin, An Efficient Seismic Retrofit for the Capodichino Viaduct, International Association for Bridge and Structural Engineering, Vancouver, Canada, 2017, pp. 144–151, https://doi.org/10.2749/vancouver.2017.0144.
[12] L. Tassinari, J. Sordet, M. Viviani, The tannery bridge: A case study in structural health monitoring and rehabilitation of structures, in: Concr. Repair Rehabil. Retrofit. IV, 1st ed, CRC Press, Leipzig, Germany, 2015, p. 204, https://doi.org/10.1201/b18972-129.

[13] R.J. Torrent, Bridge durability design after EN standards: present and future, Struct. Infrastruct. Eng. 15 (2019) 886–898, https://doi.org/10.1080/15732479.2017.1414859.

[14] E. Brühwiler, M. Bastien Masse, Strengthening the Chillon viaducts deck slabs with reinforced UHPFRC, in: IABSE Conf. Geneva 2015 Struct. Eng. Provid. Solut. Glob. Chall., IABSE, 2015, pp. 1171–1178. https://infoscience.epfl.ch/handle/20.500.14299/119560 (accessed August 28, 2024).

[15] G. Zanardo, C. Pellegrino, C. Bobisut, C. Modena, Performance evaluation of short span reinforced concrete arch bridges, J. Bridg. Eng. 9 (2004) 424–434, https://doi.org/10.1061/(ASCE)1084-0702(2004)9:5(424).

[16] A. Madni, C. Madni, S. Lucero, Leveraging Digital Twin Technology in Model-Based Systems Engineering, Systems 7, 2019, p. 7, https://doi.org/10.3390/systems7010007.

[17] C. Zhuang, J. Liu, H. Xiong, Digital twin-based smart production management and control framework for the complex product assembly shop-floor, Int. J. Adv. Manuf. Technol. 96 (2018) 1149–1163, https://doi.org/10.1007/s00170-018-1617-6.

[18] C. Ye, L. Butler, B. Calka, M. Iangurazov, Q. Lu, A. Gregory, M. Girolami, C. Middleton, A Digital Twin of Bridges for Structural Health Monitoring, 2019, https://doi.org/10.12783/shm2019/32287.

[19] T. Hielscher, S. Khalil, N. Virgona, S.A. Hadigheh, A neural network based digital twin model for the structural health monitoring of reinforced concrete bridges, Structures 57 (2023) 105248, https://doi.org/10.1016/j.istruc.2023.105248.

[20] H. Naderi, A. Shojaei, Digital twinning of civil infrastructures: current state of model architectures, interoperability solutions, and future prospects, Autom. Constr. 149 (2023) 104785, https://doi.org/10.1016/j.autcon.2023.104785.

[21] J. Heng, Y. Dong, L. Lai, Z. Zhou, D.M. Frangopol, Digital twins-boosted intelligent maintenance of ageing bridge hangers exposed to coupled corrosion–fatigue deterioration, Autom. Constr. 167 (2024) 105697, https://doi.org/10.1016/j.autcon.2024.105697.

[22] S. Honghong, Y. Gang, L. Haijiang, Z. Tian, J. Annan, Digital twin enhanced BIM to shape full life cycle digital transformation for bridge engineering, Autom. Constr. 147 (2023) 104736, https://doi.org/10.1016/j.autcon.2022.104736.

[23] Q. Lu, L. Chen, S. Li, M. Pitt, Semi-automatic geometric digital twinning for existing buildings based on images and CAD drawings, Autom. Constr. 115 (2020) 103183, https://doi.org/10.1016/j.autcon.2020.103183.

[24] A. Thelen, X. Zhang, O. Fink, Y. Lu, S. Ghosh, B.D. Youn, M.D. Todd, S. Mahadevan, C. Hu, Z. Hu, A comprehensive review of digital twin — part 1: modeling and twinning enabling technologies, Struct. Multidiscip. Optim. 65 (2022) 354, https://doi.org/10.1007/s00158-022-03425-4.

[25] D. Isailović, V. Stojanovic, M. Trapp, R. Richter, R. Hajdin, J. Döllner, Bridge damage: detection, IFC-based semantic enrichment and visualization, Autom. Constr. 112 (2020) 103088, https://doi.org/10.1016/j.autcon.2020.103088.

[26] Y. Tian, X. Zhang, H. Chen, Y. Wang, H. Wu, A bridge damage visualization technique based on image processing technology and the IFC standard, Sustainability 15 (2023) 8769, https://doi.org/10.3390/su15118769.

[27] H.V. Thakur, S.M. Nalawade, Y. Saxena, K.T.V. Grattan, All-fiber embedded PM-PCF vibration sensor for structural health monitoring of composite, Sensors Actuators A Phys. 167 (2011) 204–212, https://doi.org/10.1016/j.sna.2011.02.008.

[28] T. Moi, A. Cibicik, T. Rølvåg, Digital twin based condition monitoring of a knuckle boom crane: an experimental study, Eng. Fail. Anal. 112 (2020) 104517, https://doi.org/10.1016/j.engfailanal.2020.104517.

[29] Y. Guo, W. Liu, L. Xiong, Y. Kuang, H. Wu, H. Liu, Fiber Bragg grating displacement sensor with high abrasion resistance for a steel spring floating slab damping track, Sensors 18 (2018) 1899, https://doi.org/10.3390/s18061899.

[30] C. Ramonell, R. Chacón, H. Posada, Knowledge graph-based data integration system for digital twins of built assets, Autom. Constr. 156 (2023) 105109, https://doi.org/10.1016/j.autcon.2023.105109.

[31] Y. Schatz, B. Domer, Template matching-based method to detect bridge components in point clouds, in: Proc. 30th EG-ICE Int. Conf. Intell. Comput. Eng., London, UK, 2023. https://www.ucl.ac.uk/bartlett/construction/sites/bartlett_construction/files/3069.pdf.

[32] Industry Foundation Classes (IFC) - buildingSMART International. https://www.buildingsmart.org/standards/bsi-standards/industry-foundation-classes/, 2019 (accessed May 26, 2024).

[33] C. Boje, A. Guerriero, S. Kubicki, Y. Rezgui, Towards a semantic construction digital twin: directions for future research, Autom. Constr. 114 (2020) 103179, https://doi.org/10.1016/j.autcon.2020.103179.

[34] R. Marmo, F. Polverino, M. Nicolella, A. Tibaut, Building performance and maintenance information model based on IFC schema, Autom. Constr. 118 (2020) 103275, https://doi.org/10.1016/j.autcon.2020.103275.

[35] J. Zhu, P. Wu, X. Lei, IFC-graph for facilitating building information access and query, Autom. Constr. 148 (2023) 104778, https://doi.org/10.1016/j.autcon.2023.104778.

[36] T.H. Kwon, S.H. Park, S.I. Park, S.-H. Lee, Building information modeling-based bridge health monitoring for anomaly detection under complex loading conditions using artificial neural networks, J. Civ. Struct. Heal. Monit. 11 (2021) 1301–1319, https://doi.org/10.1007/s13349-021-00508-6.

[37] B. Domer, R. Bernardello, Interoperability: An Introduction to IFC and BuildingSMART Standards, Integrating Infrastructure Modeling, 1st ed., EPFL Press, Lausanne, Switzerland, 2023. https://www.epflpress.org/produit/1455/9782889154869/interoperability.

[38] Y. Schatz, B. Domer, Semi-automated creation of IFC bridge models from point clouds for maintenance applications, Front. Built Environ. 10 (2024), https://doi.org/10.3389/fbuil.2024.1375873.

[39] M. Pregnolato, S. Gunner, E. Voyagaki, R. De Risi, N. Carhart, G. Gavriel, P. Tully, T. Tryfonas, J. Macdonald, C. Taylor, Towards civil engineering 4.0: concept, workflow and application of digital twins for existing infrastructure, Autom. Constr. 141 (2022) 104421, https://doi.org/10.1016/j.autcon.2022.104421.

[40] Société suisse des ingénieurs et des architectes, SIA 469 - Conservation des ouvrages. https://shop.sia.ch/, 1997.

[41] U. Federale Delle Strade FEDRO, KUBA - Manufatti e Gallerie. https://www.astra.admin.ch/astra/it/home/fachleute/weitere-bereiche/fachanwendungen/kuba.html, 2024 (accessed September 4, 2024).

[42] RiSCAN PRO. https://riscan-pro.software.informer.com/, 2022 (accessed February 7, 2024).

[43] Leica Cyclone 3DR. https://leica-geosystems.com/products/laser-scanners/software/leica-cyclone/leica-cyclone-3dr, 2024 (accessed February 7, 2024).

[44] Rhino 7. https://www.rhino3d.com/7/, 2024 (accessed February 7, 2024).

[45] SketchUp 2024. https://sketchup.buildingpoint.ch/, 2018 (accessed May 30, 2024).

[46] Office Fédéral des Routes, Surveillance et Entretien des Ouvrages d'art des Routes Nationales, 2005.

[47] SCIA, Engineer 21.1. https://www.scia.net/fr/scia-engineer, 2023 (accessed May 3, 2023).

[48] Ministero delle Infrastrutture e dei Trasporti, D.M. 17/01/2018. Norme tecniche per le costruzioni (NTC 2018), Gazzetta Ufficiale, Roma, 2018 n. 29 del 14/02/2008, Supplemento ordinario n.30.

[49] Verifica Cemento Armato Stato Limite Ultimo (VCA_SLU) Version 7.8. https://gelfi.unibs.it/software/programmi_studenti.html, 2021 (accessed May 29, 2024).

[50] W.-P. Zhang, J.-P. Chen, Q.-Q. Yu, X.-L. Gu, Corrosion evolution of steel bars in RC structures based on Markov chain modeling, Struct. Saf. 88 (2021) 102037, https://doi.org/10.1016/j.strusafe.2020.102037.

[51] G. Santarsiero, A. Masi, V. Picciano, Durability of Gerber saddles in RC bridges: analyses and applications (Musmeci Bridge, Italy), Infrastructures 6 (2021) 25, https://doi.org/10.3390/infrastructures6020025.

[52] D. Mitchell, J. Marchand, P. Croteau, W.D. Cook, Concorde overpass collapse: structural aspects, J. Perform. Constr. Facil. 25 (2011) 545–553, https://doi.org/10.1061/(ASCE)CF.1943-5509.0000183.

[53] R. Storn, K. Price, A simple and efficient heuristic for global optimization over continuous spaces, J. Glob. Optim. 11 (1997) 341–359, https://doi.org/10.1023/A:1008202821328.

[54] E. Bassoli, L. Vincenzi, A.M. D'Altri, S. de Miranda, M. Forghieri, G. Castellazzi, Ambient vibration-based finite element model updating of an earthquake-damaged masonry tower: ambient vibration-based finite element model updating of an earthquake-damaged masonry tower, Struct. Control. Health Monit. 25 (2018) e2150, https://doi.org/10.1002/stc.2150.

[55] E. Bassoli, P. Gambarelli, L. Vincenzi, Human-induced vibrations of a curved cable-stayed footbridge, J. Constr. Steel Res. 146 (2018) 84–96, https://doi.org/10.1016/j.jcsr.2018.02.001.

[56] L. Vincenzi, P. Gambarelli, A proper infill sampling strategy for improving the speed performance of a surrogate-assisted evolutionary algorithm, Comput. Struct. 178 (2017) 58–70, https://doi.org/10.1016/j.compstruc.2016.10.004.

[57] L. Vincenzi, M. Savoia, Coupling response surface and differential evolution for parameter identification problems, Comput. Civ. Infrastruct. Eng. 30 (2015) 376–393, https://doi.org/10.1111/mice.12124.

[58] Y. Chikahiro, I. Ario, P. Pawlowski, C. Graczykowski, J. Holnicki-Szulc, Optimization of reinforcement layout of scissor-type bridge using differential evolution algorithm, Comput. Aided Civ. Infrastruct. Eng. 34 (2019) 523–538, https://doi.org/10.1111/mice.12432.

[59] J. Guo, Z. Guan, Optimization of the cable forces of completed cable-stayed bridges with differential evolution method, Structures 47 (2023) 1416–1427, https://doi.org/10.1016/j.istruc.2022.12.004.

[60] E.M. Abdelkader, O. Moselhi, M. Marzouk, T. Zayed, An exponential chaotic differential evolution algorithm for optimizing bridge maintenance plans, Autom. Constr. 134 (2022) 104107, https://doi.org/10.1016/j.autcon.2021.104107.

[61] Société Suisse des Ingénieurs et des Architectes, SIA 160 - Actions sur les Structures Porteuses. https://shop.sia.ch/, 1970.

[62] Société Suisse des Ingénieurs et des Architectes, SIA 162 - Ouvrages en béton Essais des Matériaux. https://shop.sia.ch/, 1968.

[63] M. Debella-Gilo, A. Kääb, Sub-pixel precision image matching for measuring surface displacements on mass movements using normalized cross-correlation, Remote Sens. Environ. 115 (2011) 130–142, https://doi.org/10.1016/j.rse.2010.08.012.

[64] B. Pan, Recent Progress in digital image correlation, Exp. Mech. 51 (2011) 1223–1235, https://doi.org/10.1007/s11340-010-9418-3.

[65] B. Pan, K. Qian, H. Xie, A. Asundi, Two-dimensional digital image correlation for in-plane displacement and strain measurement: a review, Meas. Sci. Technol. 20 (2009) 062001, https://doi.org/10.1088/0957-0233/20/6/062001.

[66] S.-H. Tung, M.-H. Shih, W.-P. Sung, Development of digital image correlation method to analyse crack variations of masonry wall, Sadhana 33 (2008) 767–779, https://doi.org/10.1007/s12046-008-0033-2.

[67] R.L. Vijaya Kumar, M.R. Bhat, C.R.L. Murthy, Evaluation of kissing bond in composite adhesive lap joints using digital image correlation: preliminary studies, Int. J. Adhes. Adhes. 42 (2013) 60–68, https://doi.org/10.1016/j.ijadhadh.2013.01.004.

[68] S. Yoneyama, A. Kitagawa, S. Iwata, K. Tani, H. Kikuta, Bridge deflection measurement using digital image correlation, Exp. Tech. 31 (2007) 34–40, https://doi.org/10.1111/j.1747-1567.2006.00132.x.

[69] S. Yoneyama, H. Ueda, Bridge deflection measurement using digital image correlation with camera movement correction, Mater. Trans. 53 (2012) 285–290, https://doi.org/10.2320/matertrans.I-M2011843.
[70] F. Chen, Z. Jin, E. Wang, L. Wang, Y. Jiang, P. Guo, X. Gao, X. He, Relationship model between surface strain of concrete and expansion force of reinforcement rust, Sci. Rep. 11 (2021) 4208, https://doi.org/10.1038/s41598-021-83376-w.
[71] Z. Li, Z. Jin, P. Wang, T. Zhao, Corrosion mechanism of reinforced bars inside concrete and relevant monitoring or detection apparatus: a review, Constr. Build. Mater. 279 (2021) 122432, https://doi.org/10.1016/j.conbuildmat.2021.122432.
[72] T. Vidal, A. Castel, R. François, Analyzing crack width to predict corrosion in reinforced concrete, Cem. Concr. Res. 34 (2004) 165–174, https://doi.org/10.1016/S0008-8846(03)00246-1.
[73] M. Malesa, D. Szczepanek, M. Kujawińska, A. Świercz, P. Kołakowski, Monitoring of civil engineering structures using digital image correlation technique, EPJ Web Conf. 6 (2010) 31014, https://doi.org/10.1051/epjconf/20100631014.
[74] C. Castagnetti, R.M. Cosentini, R. Lancellotta, A. Capra, Geodetic monitoring and geotechnical analyses of subsidence induced settlements of historic structures, Struct. Control. Health Monit. 24 (2017) e2030, https://doi.org/10.1002/stc.2030.
[75] MicMac. https://micmac.ensg.eu/index.php/Accueil, 2023 (accessed May 3, 2023).
[76] SAGA, System for Automated Geoscientific Analyses. https://saga-gis.sourceforge.io/en/index.html, 2023 (accessed May 3, 2023).
[77] F. Ponsi, E. Bassoli, L. Vincenzi, A multi-objective optimization approach for FE model updating based on a selection criterion of the preferred Pareto-optimal solution, Structures 33 (2021) 916–934, https://doi.org/10.1016/j.istruc.2021.04.084.
[78] Wolfram Mathematica, Modern Technical Computing. https://www.wolfram.com/mathematica/, 2024 (accessed May 29, 2024).